

https://doi.org/10.1070/QEL17420

Synthesis of fluorocarbon nanofilms on titanium using high-power KrF laser radiation

P.B. Sergeev, A.N. Kirichenko, K.S. Kravchuk, N.V. Morozov, R.A. Khmelnitskii

Abstract. **Fluorocarbon (C:F) nanofilms up to 60 nm thick are synthesised on a titanium surface. The films are obtained by annealing thin layers of fluorocarbon oil (FO) (with an area of 0.6 cm^2) in air with pulsed (80-ns) KrF laser radiation having a fluence of more than 4 J cm^{-2}. The strength of C : F nanocoatings turns out to be comparable with that of titanium and exceeds several hundred times the corresponding characteristics of Teflon F-4. The high transparency of FO indicates a possibility of using it as a cover liquid when modifying titanium surface using beams of various technological lasers.**

Keywords: *synthesis of nanofilms, C : F nanofilms, titanium, fluorocarbon oil, KrF laser, laser radiation.*

1. Introduction

Teflons are known to have unique physicochemical properties, a fact determining the very wide range of their application, in particular, as films and coatings [1, 2]. The discovery of graphene (Gr) and (later) fluorographene (FGr) [3] attracted the attention of researchers to these materials and their multilayer varieties with thicknesses in the nanometre range. The intensity of studying fluorographenes is characterised by the number of cited publications [3], which already exceeds 830 [4]. However, graphene and fluorographene are structures with a strictly specified carbon lattice. The carbon structure and, therefore, properties of fluorocarbon (C:F) nanofilms and coatings differ from those of fluorographene [5]. The characteristics of nanofilms depend strongly on the initial material and the way of their preparation, as well as on the material and structure of the substrates they were grown on. In essence, each new nanocoating fabrication technology gives rise to new characteristics of both the initial materials and the substrate surfaces. The strength characteristics of C:F nanocoatings may also change significantly: from the level of basic Teflon F-4 with Young's modulus of 4×10^8 Pa [1, 6] to extremely high values of 3×10^{11} Pa for FGr [3]. All these factors determine the importance of searching for new ways to synthesise fluorocarbon nanocoatings.

P.B. Sergeev, N.V. Morozov, R.A. Khmelnitskii Lebedev Physical Institute, Russian Academy of Sciences, Leninsky prosp. 53, 119991 Moscow, Russia; e-mail: sergeevpb@lebedev.ru;
A.N. Kirichenko, K.S. Kravchuk Technological Institute of Superhard and New Carbon Materials, ul. Tsentral'naya 7a, 108840 Troitsk, Moscow, Russia

Received 18 August 2020; revision received 27 September 2020
Kvantovaya Elektronika **50** (12) 1173–1178 (2020)
Translated by Yu.P. Sin'kov

Even by 2008, there were a number of publications on the synthesis of Teflon nanofilms with thicknesses from 1.5 to ~100 nm on different substrates, which was performed by depositing polymer from its solution in liquid or supercritical CO_2 [6]. It was noted that these nanofilms retained the molecular structure of fluoropolimer of the $(CF_2)_n$ type, but their self-organisation in supramolecular structures changed. These structures depended strongly on the type and quality of substrates, as well as on many other deposition parameters. The physicochemical properties of these nanofilms were comparable with those of conventional (more bulky) Teflon F-4 structures.

The discovery of unique characteristics of fluorographene stimulated studies of the properties of C:F nanofilms synthesised by different methods of chemical and physical vapour deposition (CVD technologies) [7–9]. A facilitating factor was the existence of technological equipment in many laboratories dealing with various carbon and other films and coatings [8–12]. Among others, a combined technique of synthesising a multilayer FGr was used, in which a carbon (C) nanofilm up to 10 nm thick is first synthesised by a plasma-chemical method and then its fluorination is performed [13]. The mechanical properties of this multilayer FGr should be only a little worse than those of their carbon base, as in the case of FGr and Gr. The variation of the strength properties of synthesised C nanofilms in a very wide range [14] indicates a possibility of growing very strong C:F nanofilms. Nevertheless, however important it is, the question about the ways of their synthesis remains open.

CVD technologies include laser-assisted methods for synthesising nanofilms and coatings [12, 15–21]. In particular, unique excimer electron-beam lasers (EBLs) with energies of 10 J or higher in a pulse and pulse durations of ~100 ns can be used to this end. For example, it was shown in [22] that, exposing a transformer-oil layer on the output surface of KU-1 glass substrates to two KrF EBL pulses (λ = 248 nm), one can form a hydrocarbon film up to 40 nm thick. The process was performed in air according to the scheme of laser radiation (LR) supply to a glass/liquid interface through the glass. This scheme is fairly simple but has a limitation: the substrate material must be transparent for LR. There is also a scheme with LR supply to an interface between two media (e.g., metal/liquid) through a liquid; it is often used in ablation [23–28]. In this case, the liquid must be transparent for LR. For the short-wavelength excimer laser radiation with intensities up to 100 MW cm^{-2}, it is rather difficult to draw any conclusions about the transparency of liquid on the surfaces processed because of the formation of laser plasma under these conditions. In this context, the applicability of the scheme for synthesising coatings and modifying the surface of

metals using excimer EBLs can be proven only in experiments.

The purpose of this study was to establish experimentally the possibility of forming fluorocarbon nanofilm coatings on titanium using high-power KrF EBL radiation. It was proposed to synthesise a C : F nanofilm by precipitating products from the fluorocarbon laser plasma formed near the metal surface. The results of the first favourable realisation of this idea are presented below. Titanium was chosen as a base because of the potential good prospects of the new coating specifically for this material, which is widely used in modern technologies and medicine.

2. Experimental

As was noted above, a necessary condition for successful laser modification of metal surface under a liquid layer is the maximally possible transparency of a liquid cover material for LR. An important technological requirement is the simplicity of cover layer deposition. With allowance for these requirements and experimental results of [22], fluorocarbon oil (FO) was used for the first time as a cover material. This oil is intended for use in backing pumps. Being a dense (2.2 g cm^{-3}), highly transparent liquid, it turned out to be very convenient to handle with. Fluorocarbon oil, as well as other fluorocarbon liquids, is nontoxic and fireproof.

The spectral characteristics of FO were investigated for its more detailed characterisation. The transmission spectra $T(\lambda)$ of 0.1- and 1-cm-thick FO samples placed in quartz cells were recorded using Hitachi U 3900 (wavelength range 0.19–0.8 μm) and Cary 5000 (0.2–3.3 μm) spectrophotometers and a FSM 2201 Fourier spectrometer (1.28–12.5 μm). The transmission spectra of FO films of different thicknesses on quartz and fluorite substrates, as well as the spectra of substrates and cells, were also measured. Standard digital processing of the entire set of spectra made it possible to plot the absorption spectrum of FO [$\alpha(\lambda)$] in the range of 0.2–11 μm (Fig. 1).

The UV edge of the dependence $\alpha(\lambda)$ allows one to estimate an important characteristic of amorphous materials: the optical band gap width E_{04}. It is defined as the energy of a probe light photon at which the absorption coefficient of material (generally, in the form of a thin film) is 10^4 cm^{-1} [14, 29]. For FO, this value is attached near a wavelength of 190 nm; i.e., E_{04} = 6.4 eV, a typical value of a good dielectric.

The experimentally found FO absorption coefficient at the KrF laser wavelength (248.4 nm) is 380 ± 10 cm^{-1}. Note also that the FO absorption coefficient in the spectral range of 0.35–3.2 μm does not exceed 1 cm^{-1}, whereas in the range of 0.46–2.1 μm it is smaller than 0.1 cm^{-1}. At the CO_2 laser wavelength (10.6 μm), α = 680 cm^{-1}, a value only about twice as large as in the case of KrF laser. The plateau in the spectrum $\alpha(\lambda)$ in the range of 7.5–9 μm is due to the overrun of SPM 2201 spectrometer sensitivity limit when measuring the transmittance of a thin FO film on a fluorite substrate. Here, the transmittance was lower than 0.01; therefore, the $\alpha(\lambda)$ value within the plateau is unknown (but it *a fortiori* exceeds 1124 cm^{-1}).

Because of the strong absorption of short-wavelength LR, FO can be used as a cover liquid in the case only in the form of a thin layer. A spectral study of the FO revealed that layers with thicknesses ranging from ~10 to ~50 μm can easily be deposited on glass surfaces using a cotton-wool stick. The same FO films were also formed on titanium samples:

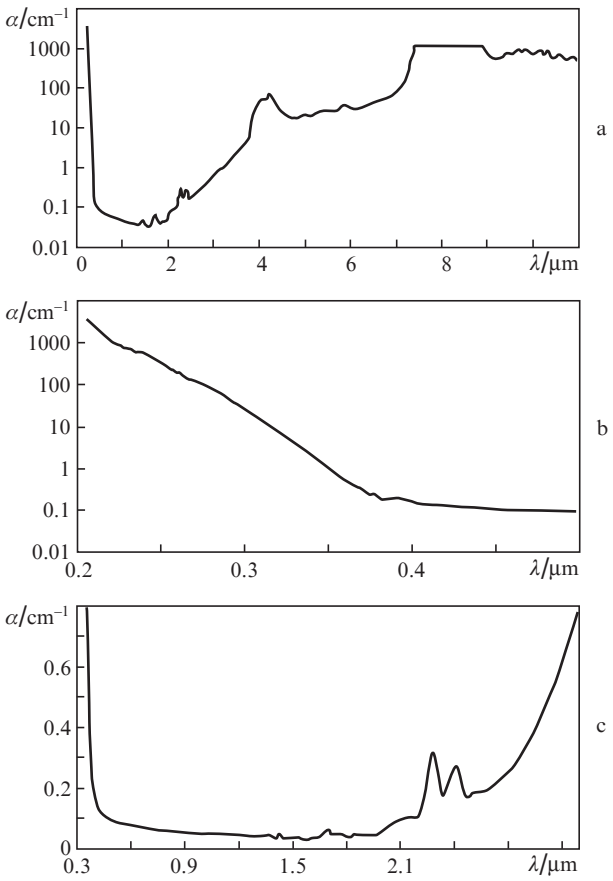

Figure 1. FO absorption spectra with different detailing.

50-μm-thick titanium foil and 0.5-mm-thick titanium plates (VT1-0). The samples were not subjected to any additional polishing.

A 10-μm-thick FO film can transmit up to 60% of incident KrF laser beam. The reflectance R of the titanium foil in use at λ = 248 nm was measured to be ~12%. According to the data of [30], where the titanium reflection spectra at photon energies in the range from 3.5 to 10 eV were reported, the reflectance for the photon energy of 5 eV (λ = 248 nm) is R = 10%. With allowance for these parameters, up to 50% of incident LR can be absorbed (disregarding nonlinear absorption) on the surface of titanium substrates coated by a 10-μm-thick FO layer.

In these experiments, as well as in [22], KrF laser radiation was generated using an electron-beam laser system ELA [31]. The LR characteristics were as follows: the energy per single 80-ns pulse was ~8 J and the radiation divergence was 10^{-2} rad. The distribution of LR energy density over the output laser window 5 cm in diameter was uniform. A plano-convex lens with a focal length of 40 cm was used to project the window image on the irradiated sample into a spot 9 mm in diameter. In our experiments the maximum fluence (F) in the spot reached 10 J cm^{-2}, when the intensity J was 125 MW cm^{-2}. The LR energy in each pulse was controlled using a calorimeter (to which part of the laser beam reflected from the focusing lens was supplied). In test pulses this channel was calibrated using another calorimeter, which measured the total LR energy behind the lens [22].

The experiments on laser synthesis of C : F nanofilms were performed with different LR fluences and different numbers

of pulses. In the first stage, there was a hindrance related to the impossibility of fast instrumental characterisation of the coatings obtained by laser irradiation. We could only rely on the visual estimation of impressions formed on titanium substrates: their shape, colour, and colour intensity. To compare the characteristics of the coatings with those of titanium samples, the latter were irradiated in air not only in the presence of FO layer but also without it.

The most important parameter in laser processing of materials is the process threshold with respect to the LR fluence or intensity. In the case of pulsed laser processing of metals, the key threshold characteristic is the fluence above which the sample surface starts melting. In our experiments melting of pure titanium plates and foil after one KrF EBL pulse was observed at $F > 1.6$ J cm^{-2}. The molten area could easily be visualised by a change in the surface blaze.

An exposure of an FO thin layer to a single LR pulse led to the formation of dark traces on the titanium foil and plates; their occurrence threshold F_m lied in the range of 4 ± 1 J cm^{-2}. The large spread for the F_m values is due to the significant spread of the thicknesses of primary FO layer and its irregularities, which smoothed out very slowly because of the high oil density. Stable occurrence of a dark film on titanium at $F > F_m$ was observed under irradiation by two LR pulses. Before the second pulse, the FO traces (retained on the surface after the first pulse) were spread over the irradiated surface of titanium sample by a dry cotton-wool stick. In this case the FO layer thickness was much smaller than 10 μm.

The main object of further study was the black coating formed on a titanium foil after the exposure of an area of FO layer to two pairs of LR pulses at $F \approx 7.5$ J cm^{-2}; oil layers were deposited before each pulse according to the above-described procedure. This coating was analysed in detail using a scanning electron microscope (SEM), a Raman spectrometer, and a nanoindenter.

Part of a titanium foil strip with a segment containing a round irradiated spot 9 mm in diameter was investigated in an electron microscope. This part was cut with conventional scissors. The typical structure of unirradiated surface of the titanium foil in use is shown (with different magnifications) in Fig. 2. One can see that the surface contains many voids and cavities of different sizes.

Figure 3a shows a pattern of the transition from the unirradiated foil area (upper part) to the area irradiated (through a FO layer) by four LR pulses (lower part with a wavy structure). Note a small width of the transition region: ~50 μm (the spot diameter is 9 mm). This focusing sharpness for the output laser window image on the irradiated foil is indicative of low LR scattering in the surface laser plasma. Note also that the height of wave ridges in the transition irradiation zone does not exceed 3 μm. They also exhibit a pronounced orientation (parallel to the irradiation boundary). This fact indicates that the waves are produced by the near-surface unloading gas flow from the laser plasma region.

The wavy structure of titanium foil surface becomes more random when approaching the laser spot centre (Fig. 3b). Here, the maximum height of wave ridges is ~5 μm. Many of these waves demonstrate pinholes produced by gas flows; the shape of their edges suggests that these flows were directed into the sample (specifically, into surface voids).

Figure 4 presents two different portions of foil cut in the region containing a black coating, which was formed after laser irradiation of the FO layer. It can be seen that the titanium surface is coated by a film ~60 nm thick; the cracks and

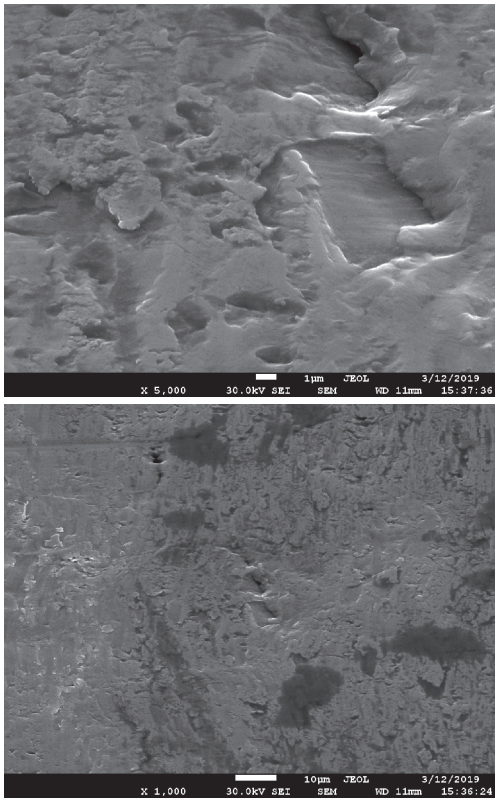

Figure 2. SEM images of the initial surface of the titanium foil with different magnifications.

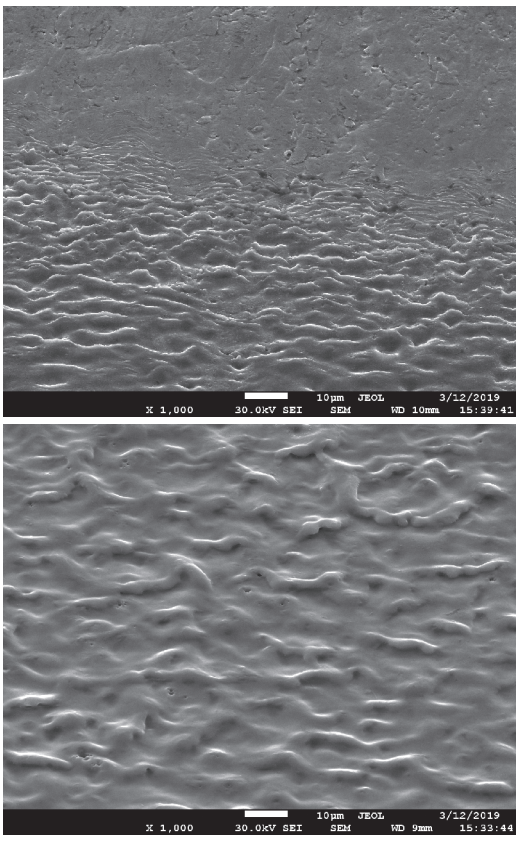

Figure 3. SEM images of the (a) boundary and (b) central region of the titanium foil area with an FO layer exposed to four KrF laser pulses.

defoliations on it are located at a distance of no more than 1000 nm from the titanium foil cut deformed by scissors. This fact is indicative of high strength characteristics of the nanofilm and its good connection with the base. A comparative X-ray fluorescence analysis of the elemental compositions of the titanium foil surface with a nanofilm synthesised on it and the adjacent region revealed that the film has a fluorocarbon composition with a C/F ratio of about 1/2.3.

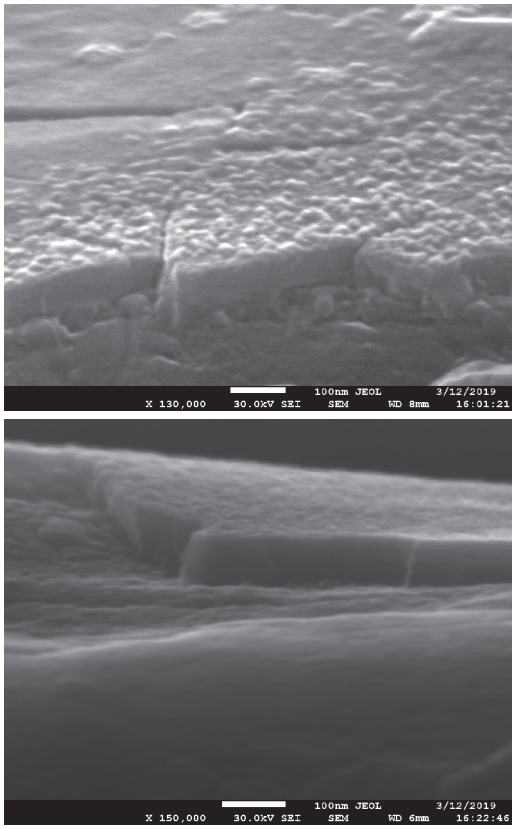

Figure 4. SEM images of two different portions of a cut of the titanium foil with a C:F nanofilm.

Direct measurements of the mechanical properties of coatings formed on a titanium foil exposed to KrF laser pulses was performed using a NanoSkan-4D nanoindenter at the Technological Institute of Superhard and New Carbon Materials. Nanoindentation was carried out according to the standard technique [32, 33]. Based on the measurement results, we plotted dependences of the sample nanohardness H on the indentation depth h and a similar dependence of normal elasticity modulus (Young's modulus) E. Figure 5 shows the corresponding data on four titanium foil samples. Two of them were irradiated in air by one or two KrF laser pulses, and two samples (coated by an FO layer) were exposed to one or four pulses. Each point in the curves was obtained by averaging the results of a series of about 10 measurements. The mean level of the measurement error over all results is characterised by the corresponding 'scatter bands' of experimental points in one of the curves.

The dependences presented in Fig. 5 show that the elastic moduli of fluorocarbon nanocoatings synthesised from FO by laser irradiation and the corresponding parameters of the titanium foil barely differ within the experimental error. It

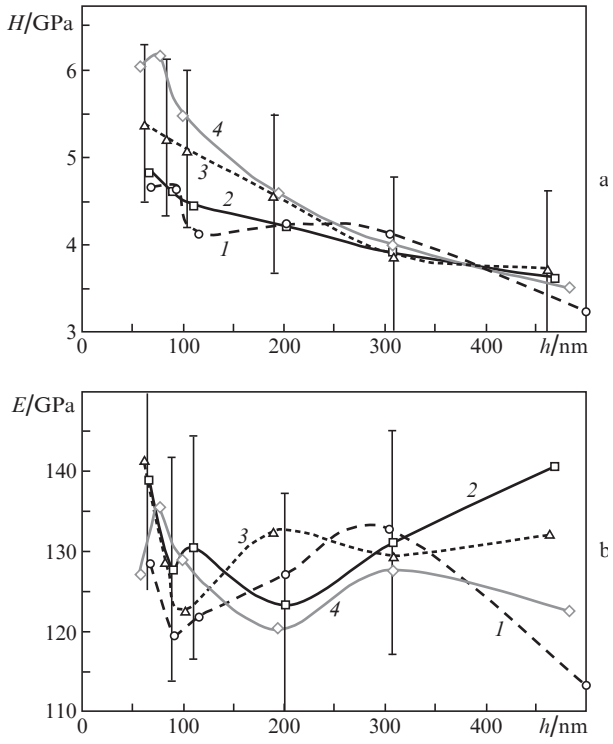

Figure 5. (a) Dependences of the nanohardness H of titanium foil samples with an FO layer on the surface, exposed to (*1*) one and (*2*) four LR pulses, and foil samples without an FO layer, exposed in air to (*3*) one and (*4*) two pulses, on the indentation depth h. (b) Similar dependences of Young's modulus E for the same samples.

can be seen that the elastic modulus (which is close to Young's modulus in the case of indentation) of the synthesised C:F nanofilm is ~130 GPa. This value is smaller than that for fluorographene by a factor of only 2.3 and exceeds elastic modulus of conventional Teflon by a factor of almost 300. It is also noteworthy that the hardness of the modified surface titanium layer about 100 nm thick (formed on the foil under laser irradiation in air) is larger by a factor of 1.5–2 than that of the bulk substrate material. A similar increase in the hardness of surface titanium layers after laser and ion treatments in air in different modes was noted previously in [34–37]. This coincidence can be considered as an additional confirmation of correctness of the performed H and E measurements.

Some of irradiated titanium samples, both with and without FO layer, were investigated by Raman spectroscopy. Measurements were performed on a Renishaw inVia Raman Microscope spectrophotometer (the United Kingdom) with an excitation laser wavelength of 532 nm. Figure 6 presents a Raman spectrum of the titanium foil with a nanofilm, obtained after exposure of FO layers to four KrF laser pulses. Almost the same spectrum was observed for the nanofilm formed as a result of single-pulse irradiation. Figure 6 shows also the Raman spectrum of the foil surface irradiated in air by two LR pulses with a fluence of 6.7 J cm^{-2} and, for comparison, the Raman spectrum of the FO used in our experiments.

The characteristic Raman bands of the titanium surface irradiated in air are located in the range $\Delta E < 1000$ cm^{-1}. Successively (in the ascending order of ΔE), these are a relatively weak band near 150 cm^{-1}, which indicates the presence

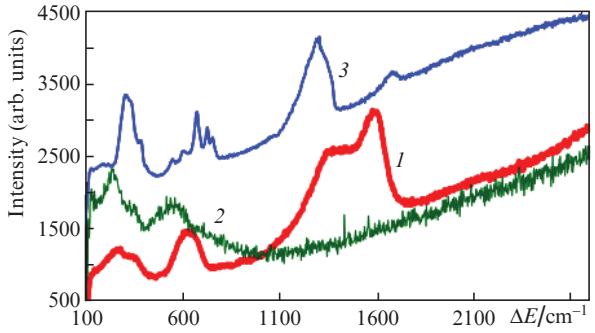

Figure 6. Raman spectra of (*1*) a C : F nanofilm on titanium and a titanium foil surface irradiated by two KrF-laser pulses (*2*) in air and (*3*) under an FOR layer; ΔE is the Raman shift.

of TiO_2 [38], and fairly strong and clearly multicomponent bands with general maxima near 250 and 570 cm^{-1}, which are very similar to the titanium nitride bands [39]. The presence of TiO_2 and nitrides on the titanium surface, with clear dominance of TiN_x, is one of the factors explaining the increase in the hardness of the corresponding layer.

The Raman spectrum of the C : F nanofilm on titanium has a two-humped structure with maxima near 1350 cm^{-1} (D band) and 1600 cm^{-1} (G band), which is characteristic of carbon lattices. These bands are fairly wide: about 160 and 130 cm^{-1}, respectively, with an intensity ratio close to unity. These characteristics indicate amorphicity of the graphite-like carbon lattice of the film under study, with a characteristic ordering length of ~15 Å [14]. In the range $\Delta E < 1000$ cm^{-1}, the C : F nanofilm exhibits two more fairly strong and, obviously, multicomponent bands: one peaking near 630 cm^{-1} and having a width of ~140 cm^{-1} and the other peaking near 300 cm^{-1}, with a width of ~200 cm^{-1}. Their nature is yet unclear to us.

The FO Raman spectrum contains four groups of bands: the first (weak) in the vicinity of 1680 cm^{-1}, the second (strong) peaking near 1300 cm^{-1}, the third (irregular) with the strongest band near 675 cm^{-1}, and the fourth (strong) peaking near 330 cm^{-1}. A comparison of these groups of FO bands with the bands of the C : F nanofilm suggests that the processes determining the transformation of the first two FO bands into the G and D bands of the nanofilm may also determine the corresponding transformation of the other two bands. This suggestion requires a further detailed study, which is, however, beyond the scope of this paper.

3. Conclusions

The main result of our study is the proof that fluorocarbon nanofilms can be synthesised on a titanium surface during irradiation of a thin (less than 10 μm) FO cover layer in air by KrF EBL pulses. The strength characteristics of the obtained C : F nanofilms are comparable with similar titanium characteristics, which exceed several hundred times the corresponding characteristics of Teflon F-4. The procedure of depositing a thin FO cover layer on titanium surfaces, as well as their subsequent annealing in air by laser radiation, is simple, convenient, and does not require any additional expensive equipment. It may serve a basis for the technology of step-by-step deposition of protective high-strength fluorocarbon nanofilm coatings on large areas of titanium products. It was shown that pure FO can be used (in view of its high transparency) as a cover liquid in the form of layers of different thickness when modifying the titanium surface by beams of practically all technological lasers with wavelengths ranging from 0.25 to 10.6 μm. FO is the first representative of a wide class of fluorocarbon liquids that can also be used as cover ones in laser processing of various materials.

Acknowledgements. We are grateful to Ya.K. Skasyrskii for the help in spectral measurements.

References

1. Baskin Z.L., Shabalin D.A., Vyrazheikin E.S., Dedov S.A. *Ross. Khim. Zh.*, **52** (3), 13 (2008).
2. Beider E.Ya., Donskoi A.A., Zhelezina G.F., Kondratov E.K., Sytyi Yu.V., Surnin E.G. *Ross. Khim. Zh.*, **52** (3), 30 (2008).
3. Nair R.R., Ren W.C., Jalil R., Riaz I., Kravets V.G., Britnell L., Blake P., Schedin F., Mayorov A.S., Yuan S., Katsnelson M.I., Cheng H.M., Strupinski W., Bulusheva L.G., Okotrub A.V., Grigorieva I.V., Grigorenko A.N., Novoselov K.S., Geim A.K. *Small*, **6**, 2877 (2010).
4. https://onlinelibrary.wiley.com/doi/abs/10.1002/smll.201001555.
5. Karlicky F., Otyepka M. *Ann. Phys.*, **526** (9-10), 408 (2014).
6. Nikitin L.N., Gallyamov M.O., Said-Galiev E.E., Khokhlov A.R., Buznik V.M. *Ross. Khim. Zh.*, **52** (3), 56 (2008).
7. Zhuk A.V., Sonnenberg N. RF Patent No. 0002608482 (Priority date 18 January, 2017).
8. Shvedov A.V., Elinson V.M., Shchur P.A., Kirillov D.V. *Vak. Tekh. Tekhnol.*, **29** (2), 36 (2019).
9. Fadeeva Yu.V., Okotrub A.V. *Zh. Strukt. Khim.*, **59** (4), 787 (2018).
10. Spitsyn B.V., Aleksenko A.E. *Zashch. Met.*, **43** (5), 456 (2007).
11. Grill A. *Diam. Relat. Mater.*, **8**, 428 (1999).
12. Konov V.I. *Quantum Electron.*, **45** (11), 1043 (2015) [*Kvantovaya Elektron.*, **45** (11), 1043 (2015)].
13. Kuan-I Ho et al. *Sci. Rep.*, **4**, 5893 (2014).
14. Robertson J. *Mater. Sci. Eng. R*, **37**, 129 (2002).
15. Gorbunov A.A., Konov V.I. *Surf. Coat. Technol.*, **47**, 503 (1991).
16. Voevodin A.A., Donley M.S. *Surf. Coat. Technol.*, **82**, 199 (1996).
17. Konov V.I., Uglov S.A. *Quantum Electron.*, **28** (4), 281 (1998) [*Kvantovaya Elektron.*, **25** (4), 291 (1998)].
18. Bol'shakov A.P., Vostrikov V.G., Dubrovskii V.Yu., Konov V.I., Kosyrev F.K., Naumov V.G., Ral'chenko V.G. *Quantum Electron.*, **35** (4), 385 (2005) [*Kvantovaya Elektron.*, **35** (4), 385 (2005)].
19. Tver'yanovich Yu.S., Man'shina A.A., Tver'yanovich A.S. *Russ. Chem. Rev.*, **81** (12), 1091 (2012) [*Usp. Khim.*, **81** (12), 1091 (2012)].
20. Lyalin A.A., Simakin A.V., Bobyrev V.A., Lubnin E.N., Shafeev G.A. *Quantum Electron.*, **29** (4), 355 (1999) [*Kvantovaya Elektron.*, **27** (1), 73 (1999)].
21. Simakin A.V., Lubnin E.N., Shafeev G.A. *Quantum Electron.*, **30** (3), 263 (2000) [*Kvantovaya Elektron.*, **30** (3), 263 (2000)].
22. Sergeev P.B., Morozov N.V., Kirichenko A.N. *Quantum Electron.*, **48** (2), 136 (2018) [*Kvantovaya Elektron.*, **48** (2), 136 (2018)].
23. Barmina E.V., Serkov A.A., Shafeev G.A. *Quantum Electron.*, **43** (12), 1091 (2013) [*Kvantovaya Elektron.*, **43** (12), 1091 (2013)].
24. De Bonis A., Sansone M., D'Allesio L., Galasso A., Santagata A., Teghil R. *J. Phys. D: Appl. Phys.*, **46**, 445301 (2013).
25. Lam J., Amans D., Chaput F., Diouf M., Ledoux G., Mary N., Masenelli-Variot K., Motto-Ros V., Dujardin C. *Phys. Chem. Chem. Phys.*, **16**, 963 (2014).
26. Ionin A.A., Kudryashov S.I., Levchenko A.O., Makarov S.V., Saraeva I.N., Rudenko A.A., Butsen' A.V., Burakov V.S. *JETP Lett.*, **106** (4), 268 (2017) [*Pis'ma Zh. Eksp. Teor. Fiz.*, **106** (4), 247 (2017)].
27. Kudryashov S.I., Samokhvalov A.A., Nastulyavichus A.A., Saraeva I.N., Mikhailovskii V.I., Ionin A.A., Veiko V.P. *Materials*, **12**, 562 (2019).
28. Kochuev D.A., Khor'kov K.S., Abramov D.V., Arakelyan S.M., Prokoshev V.G. *Poverkhn.: Rentgenovskie, Sinkhrotronnye Neitr. Issled.*, (12), 81 (2018).

29. Theye M.-L., Paret V., Sadki A. *Diam. Rel. Mater*., **10**, 182 (2001).
30. Ivanov S.N., Loktionov E.Yu., Protasov Yu.Yu. *Vestn. Mosk. Gos. Tech. Univ. im. N.E. Baumana, Ser. Estestv. Nauki*, (1), 25 (2010).
31. Sergeev P.B. *J. Sov. Laser Res*., **14** (4), 237 (1993).
32. Useinov A.S., Kravchuk K.S., Rusakov A.A., Krasnogorov I.V., Kuznetsov A.P., Kazieva T.V. *Phys. Procedia*, **72**, 194 (2015).
33. Useinov A.S., Rusakov A.A., Yakovlev V.I., Gladkikh E.V. *Nanoindustriya*, (1), 66 (2020).
34. Morozova E.A., Muratov V.S. *Vestn. Tomsk Gos. Univ*., **15** (3), 862 (2010).
35. Gorunov A.I., Gil'mutdinov A.Kh. *Izv. Vyssh. Uchebn. Zaved., Ser. Poroshk. Metall. Funct. Pokrytiya*, **4**, 40 (2015).
36. Lavisse L., Berger P., Cirisan M., Jouvard J.M., Bourgeois S., Marco de Lucas M.C. *J. Phys. D: Appl. Phys*., **42**, 245303 (2009).
37. Chernov I.P., Beloglazova P.A., Berezneeva E.V., Kireeva I.V., Pushilina N.S., Remnev G.E., Stepanova E.N. *Tech. Phys*., **60** (7), 1039 (2015) [*Zh. Tekh. Fiz*., **85** (7), 95 (2015)].
Shul'ga Yu.M., Matyushenko D.V., Golyshev A.A., Shakhrai D.V., Molodets A.M., Kabachkov E.N., Kurkin E.N., Domashnev I.A. *Tech. Phys. Lett*., **36** (9), 841 (2010) [*Pis'ma Zh. Tekh. Fiz*., **36** (18), 26 (2010)].
38. Spengler W., Kaiser R., Christensen A.N., Muller-Vogt G. *Phys. Rev. B*, **14**, 1095 (1978).